Optics Communications 285 (2012) 113–117

Contents lists available at SciVerse ScienceDirect

Optics Communications

journal homepage: www.elsevier.com/locate/optcom

Weak mode coupling measurement with EMD-based method in polarization-maintaining fibers

Hongxia Zhang *, Wenting Ye, Xinwei Chen, Yaguang Ren, Dagong Jia, Guoqiang Wen, Yimo Zhang

College of Precision Instrument & Opto-electronics Engineering, Tianjin University, Tianjin 300072, PR China
Key Laboratory of Opto-electronics Information Technology (Tianjin University), Ministry of Education, Tianjin 300072, PR China

ARTICLE INFO

Article history:
Received 4 May 2011
Accepted 7 September 2011
Available online 25 September 2011

Keywords:
Polarization-maintaining fiber
White light interferometry
Empirical mode decomposition (EMD)
Polarization coupling measurement (PCM)
Discrete wavelet transform (DWT)

ABSTRACT

The intensity and position of coupling points in polarization-maintaining fibers (PMFs) caused by force and twist can be effectively detected by Polarization Coupling Measurement (PCM). The sensitivity of detection will decrease due to the movement of scanning Michelson interferometer. To detect the weak coupling point, an EMD-based method is proposed in this paper. The experimental results illustrate that the EMD-based method can suppress the noise and improve the SNR effectively. The DWT method is also performed for a comparative study. The results show that the EMD-based method is effective and applicable for PCM and the coupling point can still be detected when the intensity is as weak as −70 dB.
© 2011 Elsevier B.V. All rights reserved.

1. Introduction

Distributed fiber optics sensors, which employ white-light interferometry (WLI) based on polarization mode coupling detection in polarization maintaining fibers (PMFs), are widely used in the measurement of strain, twist, temperature, and many other physical parameters[1–5]. The intensity and position of the coupling points can be effectively detected with high spatial resolution and wide dynamic range in the polarization coupling measurement (PCM)[6].

However, the signal noise ratio (SNR) and the detection sensitivity of PCM will decrease due to the nonlinear error caused by the vibration of the step motor and the movable mirror in the scanning Michelson interferometer. Therefore, it is difficult to detect the weak coupling points because they will be submerged in noise. Some methods have been proposed to improve the SNR. Phase modulation or differential signal detection can be employed for weak coupling measurement [7–9], however, the complexity of PCM would be increased. Some data processing methods such as band-pass filtering [10], the Wigner–Ville distribution and the wavelet transforms [11] have also been reported in other measurement systems to minimize the influence of noise. Setting a particular cutoff frequency in the Fourier smoothing filtering can separate the signal from the noise if the signal varies slowly compared to the noise. But the non-stationary and nonlinear signal cannot be effectively handled with the above methods. The empirical mode decomposition (EMD) is a high efficient technique for processing nonlinear and non-stationary signals because the procedure is data-driven, adaptive and not restricted by linearity or priori conception [12–18].

In the paper, the EMD decomposition is used to measure the weak coupling points in the PCM. The effectiveness of the EMD-based method is verified in experiments.

2. Weak mode coupling measurement in PCM

The scheme of the PCM is shown in Fig. 1. The detailed experiment setup is described by X. Chen et al [19]. The SLD emits the broadband light and an in-line polarizer is fused and spliced to the PMF. The output light from the fiber is collimated, passed through a rotatable half wave plate and an analyzer, and then is injected into the scanning Michelson interferometer. The interference signal is detected with the PD.

The output intensity of the spectral interferogram can be expressed as [20]:

$$I_{out} = I_o\left\{1 + \exp\left[-(d/L_c)^2\right]\cos(k_o d) + \sqrt{h-h^2}\exp\left(-L_c^2 d^2/2\right)\cos(\Delta\beta l - k_o d)\right\} \quad (1)$$

* Corresponding author at: College of Precision Instrument & Opto-electronics Engineering, Tianjin University, Tianjin 300072, PR China. Tel./fax: +86 22 27403147.
E-mail address: hxzhang@tju.edu.cn (H. Zhang).

0030-4018/$ – see front matter © 2011 Elsevier B.V. All rights reserved.
doi:10.1016/j.optcom.2011.09.016

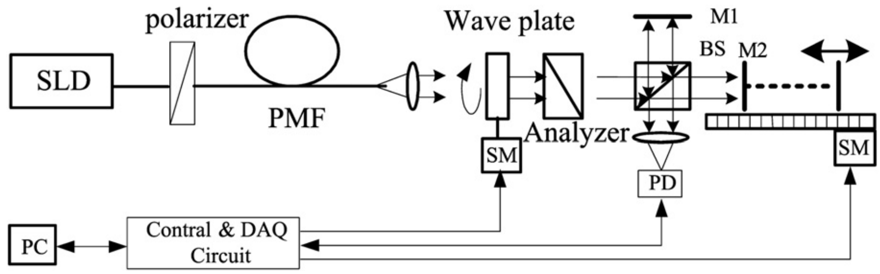

Fig. 1. System schematic of the PCM. (SLD: superluminescent diode, BS: beam splitter, PD: photodiode, SM: step motor. M1: stable mirror, M2: movable mirror).

where I_o is the direct current (DC) component of the interference, L_c is the coherence length of the light source, d is the optical path difference (OPD) of the scanning Michelson interferometer, k_o is the wave number in free space, h is the coupling intensity parameter, l is the fiber length between the coupling point and the output end of the fiber, and $\Delta\beta$ are the propagation constant differences of the two eigenmodes.

The movement of the SM will produce vibration of the movable mirror M2 in the Michelson interferometer, which will probably cause the fluctuation of OPD. So the intensity of the practical interferogram can be described as:

$$
\begin{aligned}
I_{out} = I_o \Big\{ 1 + \exp\left[-((d + rand(\Delta d))/L_c)^2\right] \cos(k_o(d + rand(\Delta d))) \\
+ \sqrt{h - h^2} \exp\left(-\left(L_c^2 (d + rand(\Delta d))^2\right)/2\right) \cos(\Delta\beta l - k_o(d + rand(\Delta d))) \Big\}
\end{aligned}
\tag{2}
$$

where $rand(\Delta d)$ is the OPD fluctuation caused by the Michelson interferometer.

The practical acquired interferogram is shown in Fig. 2. There is sudden-change structure in the detailed drawing which shows the nonlinear and non-stationary feature existing in the signal.

The relationship between the intensity of polarization mode coupling and the output intensity of the spectral interferogram can be expressed as [20]:

$$
h = 10 \log\left(I_{cf}/I_{main}\right)^2 \tag{3}
$$

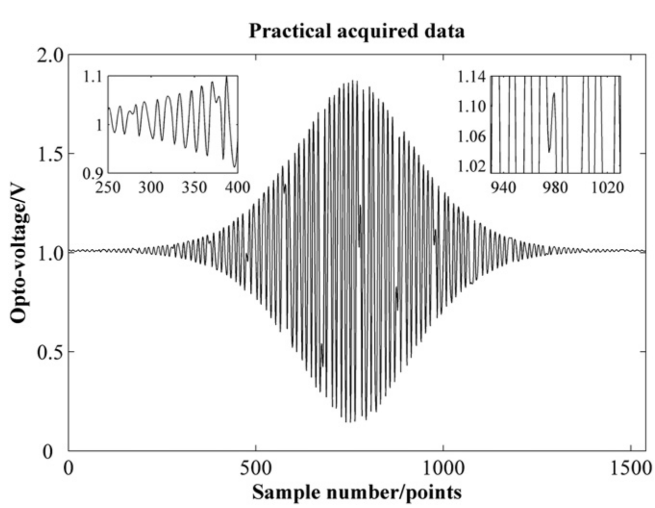

Fig. 2. Practical acquired interferogram.

where I_{main} represents the amplitude of interference fringe when the OPD is zero and I_{cf} is the amplitude of zero order fringe in the interference packet.

3. The EMD-based method

Based on the signal characteristics of PCM, the EMD-based method combined with data averaging is proposed. The process is shown in Fig. 3 and the specific steps are described as follows:

Step1: Acquire opto-voltage data of the output interferogram from the PCM.

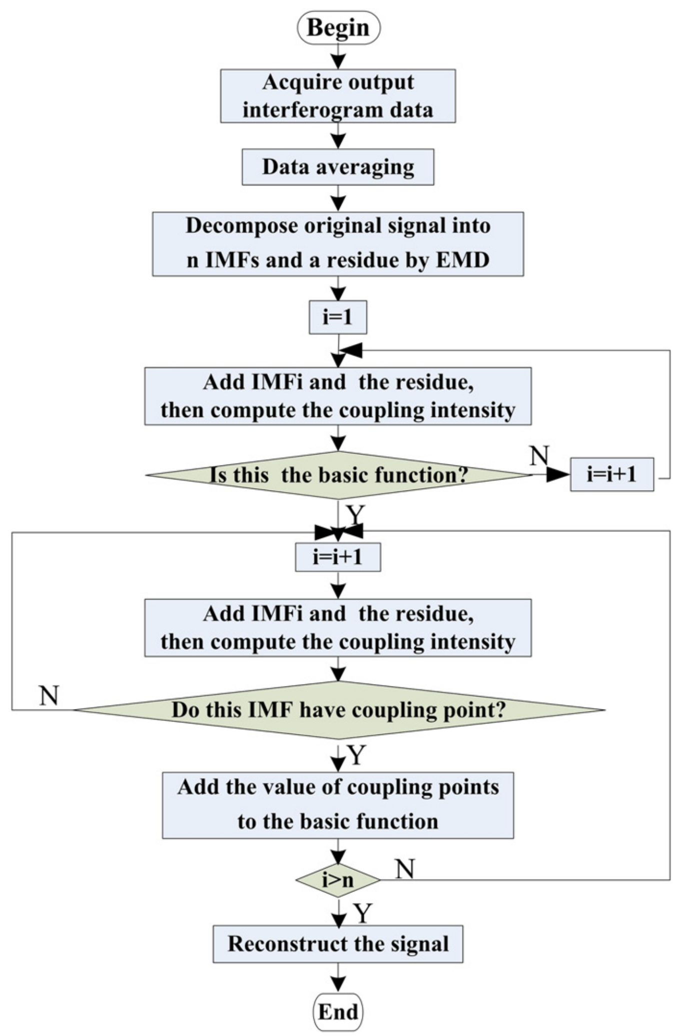

Fig. 3. EMD-based process.

Step2: Employ the data averaging method to suppress the random noise effectively.

Step3: Decompose the noisy signal with the EMD algorithm. Thus the original noisy signal $x_0(t)$ can be expressed as follows:

$$x_0(t) = \sum_{i=1}^{n} c_i(t) + r(t) \quad (1 \le i \le n) \tag{4}$$

where $c_i(t)$ is the intrinsic mode function (IMF), $r(t)$ is the residue which presents the overall trend, n, i is the number and the order of the IMF respectively.

Step4: Find the basic function $b(t)$. Add IMF1 to the residue and compute the coupling intensity marked as $x_1(t)$. If $x_1(t)$ is greater than the standard deviation (SD) of the signal, $x_1(t)$ is the basic function. If not, then add IMF2 to the residue and judge if $x_2(t)$ is the basic function. Just repeat the process in turn until the basic function $b(t)$ is found.

Step5: Recognize the coupling points and reconstruct the signal. Add the rest IMFs and the residue in turn separately. If the coupling intensity is greater than the SD of the signal, record the coupling point and discard the duplicate one. Finally, add all the coupling points to the basic function $b(t)$ and reconstruct the signal.

4. Experiments

The SLD-101 of General Photonics Company emitting at 1328 nm was used as the light source. Its spectrum followed a Gaussian distribution and the spectral half-width was approximately 36.5 nm. The USB 6251 of National Instrument was used for data acquisition. The scanning speed of the step motor with M2 was 0.75 mm/s. The light power is changed to verify the effectiveness of the EMD-based method. In the experiment, the acquired opto-voltage of photodiode varies from 0.55 V to 5.25 V and a PMF with four coupling points has been tested. The DWT methods have also been compared and analyzed.

The experiment results are shown in Fig. 4. It illustrates the SNR improves with the EMD-based and DWT methods when the detective opto-voltage varies. The blue curve is the SNR of the original noisy signal ranging 53.91 dB–69.94 dB and the green one represents the SNR acquired with EMD-based method ranging 70.83 dB–84.36 dB. Based on DWT with db8 of 5 layers with global threshold, the red curve shows SNR of 72.75 dB–83.16 dB. Based on DWT with coif5 of 4 layers with 'minimaxi' threshold, the purple curve shows SNR of 72.28 dB–82.78 dB. Based on DWT with coif3 of 3 layers with 'rigrsure' threshold, the pink curve shows SNR of 71.11 dB–78.09 dB. Based on DWT with sym4 of 3 layers with hierarchical threshold of 1.5, the gray curve shows SNR of 70.84 dB–81.78 dB. Among these DWT methods, the DWT with db8 is the most suitable for the PCM.

The scanning speed of the step motor is 0.75 mm/s and the opto-voltage is 3.79 V. The coupling intensity results with different methods are shown in Fig. 5, where A is the coupling interference fringe when the OPD is zero. B, C, D, E are the coupling points in the PMF and the coupling intensities are −37.97 dB, −52.30 dB, −46.22 dB and −35.49 dB respectively. Fig. 5(a) is the original coupling intensity and the B, D, E three coupling points can be recognized, so coupling point whose coupling intensity is weaker than −50 dB can't be detected. Fig. 5(b) is the reconstructed signal using the proposed EMD-based method. The original signal is processed into 16 IMFs and a residue by the EMD-based method. The coupling detection sensitivity is better than −70 dB. The DWT algorithms with different mother functions have also been compared. In Fig. 5(c), the coupling intensities of B, C, D, E decrease to −44.05 dB, −60.45 dB, −52.13 dB and −40.92 dB respectively which are the incorrect diagnosis of coupling points. In Fig. 5(d)(f), the sensitivity of the coupling points detection are both worse than that with EMD-based method. In Fig. 5(e), the noise level between A and B is higher. After EMD-based de-noising and reconstruction, the SNR of the signal is improved from 68.10 dB to 82.85 dB. In Fig. 5(c)(d)(e)(f), the SNR increases to 79.64 dB, 76.23 dB, 79.88 dB, 76.23 dB respectively. A satisfactory performance for noise suppressing has been implemented by EMD-based method.

The method has also been employed with 50 Hz interference, which will induce more fluctuation and disturbance. Fig. 6 shows the de-noising performance. Fig. 6(a) is the coupling intensity embedded in 50 Hz noise and the detection sensitivity is only −30 dB. Fig. 6(b) is the reconstructed signal with EMD-based method. Fig. 6(c) is the result with DWT of db8 which is the best method in Fig. 5. Obviously, the DWT-based method is out of service, while the EMD-based method is still capable of reducing noise and preserving signal information. Several weak coupling points can also be directly detected with the EMD-based method. The coupling intensity of the noisy signal attains a SNR of 35.17 dB and the SNR improved by 31.43 dB with EMD-based method.

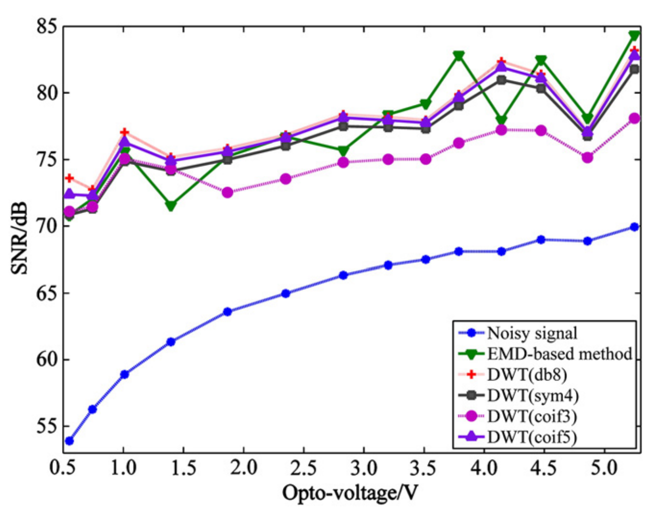

Fig. 4. Detective opto-voltage vs SNR.

5. Discussions

The PCM is influenced by the noise and the acquired signal shows nonlinear characteristics. EMD acts as a set of filters and decomposes the original signal from high frequency to low frequency in their turn. The SNR improvement in Fig. 4 shows that the EMD-based method can suppress the noise effectively. The coupling point can still be detected when the intensity is as weak as −70 dB.

The de-noising performance between EMD-based and DWT methods has been compared. Different mother functions of DWT have been tested and the SNR differs 5 dB. Based on DWT with coif5, incorrect diagnoses will come up because the coupling intensity of the coupling points is smaller than the true value. In these DWT methods, db8 has the best performance. However, the selection of mother function in DWT is influenced by the characteristic of the original signals. So when we are dealing with unknown signals or nonlinear data, the EMD-based method is more simple and timesaving. In addition, when the signal is embedded in 50 Hz interference, the EMD-based method can identify the coupling points effectively

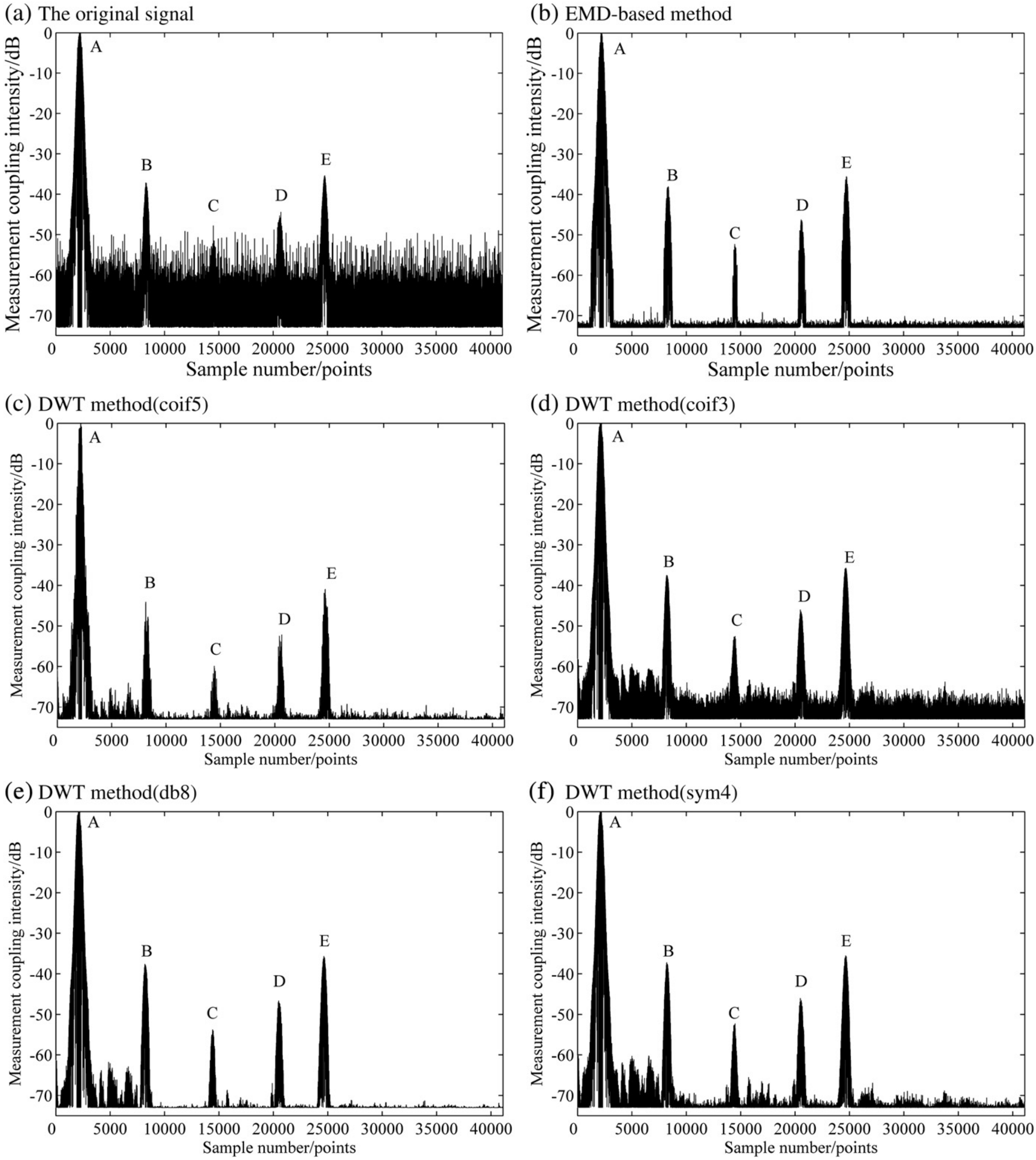

Fig. 5. Coupling intensity measurement with EMD-based and DWT methods.

while the DWT is out of service. In conclusion, the EMD-based method is better than DWT method in the PCM.

6. Conclusions

In this paper, an EMD-based method has been proposed and presented in PMF with PCM. The improvement in the SNR indicates the validity of the noise cancelation. The coupling point can still be detected when the intensity is as weak as −70 dB. The DWT method is also performed for a comparative study.

Acknowledgements

This work was supported by National Basic Research Program of China (973 Program) under Grant No. 2010CB327806.

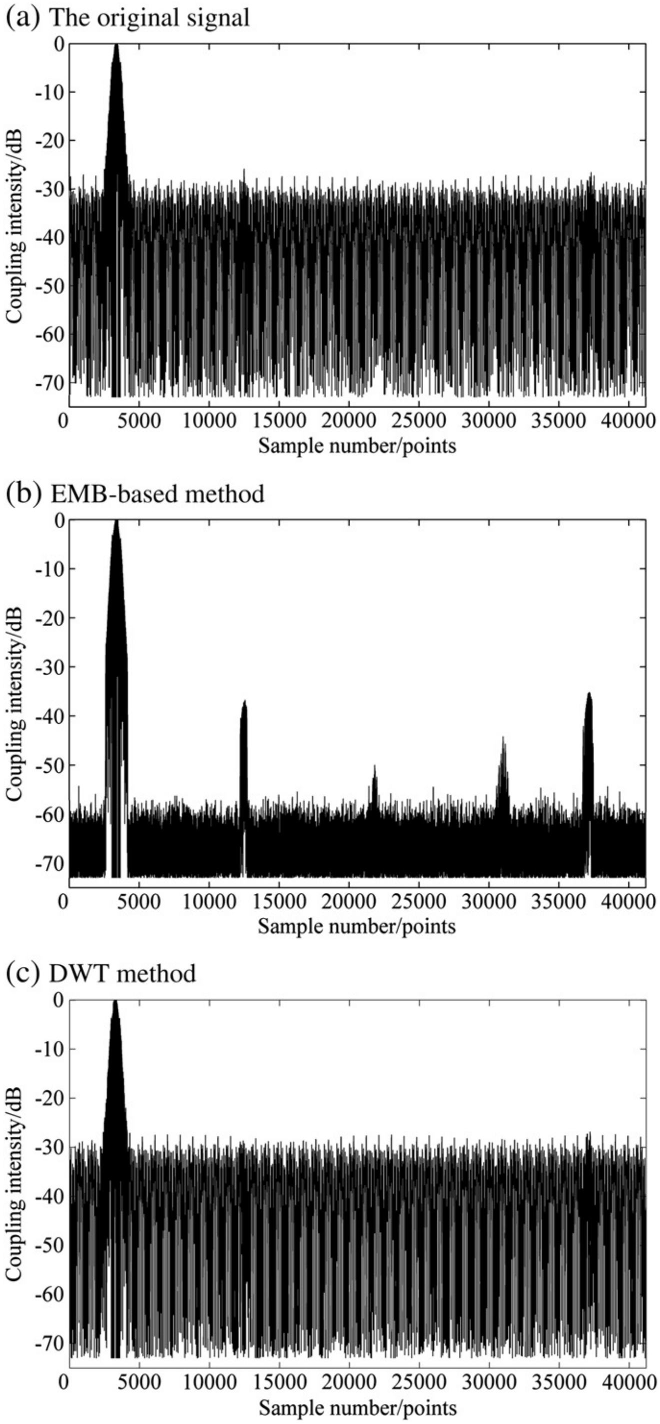

Fig. 6. Coupling intensity with 50 Hz interference.

References

[1] T. Saida, K. Hotate, IEEE Photonics Technology Letters 9 (1997) 484.
[2] L. Yuan, L. Zhou, W. Jin, Optics Letters 25 (2000) 1074.
[3] Denis Donlagic, Miran Lesic, Optics Express 14 (2006) 10245.
[4] Shiping Chen, B.T. Meggitt, Andrew William Palmer, Kenneth Thomas V. Grattan, R.A. Pinnock, Journal of Lightwave Technology 15 (1997) 261.
[5] Gabriela Statkiewicz, Tadeusz Martynkien, Wacław Urbanczyk, Optics Communications 241 (2004) 339.
[6] W. Jing, Y. Zhang, G. Zhou, F. Tang, H. Li, Optics Express 10 (2002) 685.
[7] Ju-Yi Lee, Der-Chin Su, Optics Communications 198 (2001) 333.
[8] K. Takada, J. Noda, K. Okamoto, Optics Letters 11 (1986) 680.
[9] W. Jing, Y. Zhang, G. Zhou, H. Zhang, Z. Li, X. Man, Optics Express 10 (2002) 972.
[10] V.X. Afonso, W.J. Tompkins, T.Q. Nguyen, K. Michler, S. Luo, IEEE Engineering in Medicine and Biology 15 (1996) 37.
[11] X. Wang, Y. Zi, Z. He, Mechanical Systems and Signal Processing 25 (2011) 285.
[12] Norden E. Huang, Zheng Shen, Steven R. Long, Manli C. Wu, Hsing H. Shih, Quanan Zheng, Nai-Chyuan Yen, Chi Chao Tung, Henry H. Liu, Proceedings of the Royal Society of London Series A 454 (1998) 903.
[13] Norden E. Huang, Man-Li C. Wu, Steven R. Long, Samuel S.P. Shen, Wendong Qu, Per Gloersen, Kuang L. Fan, Proceedings of the Royal Society of London Series A 459 (2003) 2317.
[14] Yannis Kopsinis, Stephen McLaughlin, IEEE Transactions on Signal Processing 57 (2009) 1351.
[15] Y. Zhang, Y. Gao, L. Wang, J. Chen, X. Shi, IEEE Transactions on Biomedical Engineering 54 (2007) 1631.
[16] Oumar Niang, Éric Deléchelle, Jacques Lemoine, IEEE Transactions on Signal Processing 58 (2010) 5612.
[17] Alejandro Federico, Guillermo H. Kaufmann, Optics Communications 267 (2006) 287.
[18] Shih-Lin Lin, Pi-Cheng Tung, Norden E. Huang, Physical Review E 79 (2009) 066705–1.
[19] X. Chen, H. Zhang, D. Jia, T. Liu, Y. Zhang, Journal of Modern Optics 58 (2011) 26.
[20] T. Xu, W. Jin, H. Zhang, K. Liu, D. Jia, Y. Zhang, Optical Fiber Technology 15 (2009) 83.